ARTICLE NO. 79-0801R

J80-215

Assumed Stress Finite Element Analysis of Through-Cracks in Angle-Ply Laminates

40003
40005

T. Nishioka* and S. N. Atluri†
Center for Advancement of Computational Mechanics, Georgia Institute of Technology, Atlanta, Ga.

In the present paper a new assumed stress finite element method, based on a complementary energy method, is developed for the analysis of cracks in angle-ply laminates. In this procedure, the fully three-dimensional stress state (including transverse normal and shear stresses) is accounted for; the mixed-mode stress and strain singularities, whose intensities vary within each layer near the crack front, are built into the formulation a priori; the interlayer traction reciprocity conditions are satisfied a priori; and the individual cross-sectional rotations of each layer are allowed; thus resulting in a highly efficient and cost-effective computational scheme for practical application to fracture studies of laminates. Results obtained from the present procedure, for the case of an uncracked laminate under bending and for the case of a laminate with a through-thickness crack under far-field tension, their comparison with other available data, and pertinent discussion, are presented.

Introduction

AN accurate three-dimensional stress analysis of angle-ply laminates with cracks and/or holes, as opposed to the use of simpler "classical laminates plate theories," is often times mandatory to understand 1) the complicated feature of the often-observed non-self-similar crack growth in symmetric angle-ply laminates; 2) the subcritical damage in the form of matrix crazing, splitting, and delamination that is observed to precede final failure in a laminate; and 3) to more clearly understand the hole-size effects in a laminate.

Quasi-three-dimensional analyses of cracked angle-ply laminates, with the assumption of 1) zero transverse normal stress in the laminate, 2) perfect bonding between lamina, and 3) each laminate being treated as a homogeneous anisotropic medium, were recently reported by Wang et al.[1] The procedures in Ref. 1 do not account, a prior, for the mixed-mode stress and strain singularities near the crack front, and hence involve expensive computations using very fine finite element meshes of conventional, polynomial-based elements. From these very-fine-mesh finite element solutions, even though one may obtain high stress-gradient solutions in the limit, it is often inconvenient to extract the results for mixed-mode stress intensity factors near the crack front. Also, the finite element that is used in Ref. 1 is the multilayer assumed-stress hybrid element originally developed by Mau et al.[2] for the analysis of uncracked laminates. In the procedure of Ref. 2, a stress field is assumed independently in each layer and interlayer traction reciprocity conditions are enforced through the method of Lagrange multipliers, which necessarily complicates the formulation and results in expensive computations. Also, since the stresses are independently assumed in each layer, the computational procedure in Refs. 1 and 2 become prohibitively expensive for a large number of layers. Finally, it is noted that the effects of transverse normal stress σ_{33} (x_3 being the thickness-coordinate of the laminate) are ignored in Refs. 1 and 2.

Later, to study the effects of σ_{33}, Wang et al.[3] employed a finite element model wherein each layer of the laminate was modeled by fully three-dimensional assumed stress hybrid elements, whose formulation was given earlier by Pian.[4] Since mixed-mode stress and strain singularities were not embedded a priori in these elements, Wang et al.[3] employed a very fine three-dimensional finite element mesh. For instance, in the analysis of a through-thickness crack in a 90°/0°/0°/90° laminate under tension, they employed a two-stage solution technique. In the first stage, a three-dimensional finite element mesh of $9\times18\times2$ (2 being in x_3 direction) with 1710 degrees-of-freedom (d.o.f) was used; while the inner mesh, whose boundary conditions were determined from the coarse mesh solution, consisted of $(11\times19\times4)$ three-dimensional elements with 3600 d.o.f.

The above discussion suggests a need for a more economical solution method for cracks in laminates, which at the same time should yield information, directly, concerning the mixed-mode stress-intensities near the crack-front. The development of such a method is one of the primary objectives of the present paper. In the present procedure, the fully three-dimensional stress-state, including σ_{33}, is accounted for; the mixed-mode stress and strain singularities, whose intensities vary within each layer near the crack-front, are built into the formulation a priori; and interlayer traction reciprocity conditions are satisfied a priori; thus resulting in a highly efficient numerical scheme for practical application to fracture studies of laminates. Results are presented for two problems: 1) bending of a simply supported (0°/90°/0°) laminate under a sinusoidal transverse load, for which an exact three-dimensional solution is available,[5] and 2) through-thickness edge crack in a (90°/0°/0°/90°) laminate under uniform tension, for which an independent numerical solution is available.[3] Comparing the present results with those in Refs. and 2, 3, and 5, the possible advantages of the present method are noted.

Description of the Present Analysis Procedure

Let the laminate consist of k layers, $i=1,2,...k$; and let the planar domain of the laminate be divided into M finite elements, $n=1,...M$. We consider here that each finite element consists of the entire stack of layers in the laminate. Let V_n^i be the volume of the ith layer within the nth element; ∂V_n^i be the boundary of V_n^i; S_{on}^i be the part of ∂V_n^i where tractions are prescribed. Further, we use the notation that ($\sim$) under a symbol denotes a vector and ($\approx$) under a symbol denotes a matrix. Let $\underset{\sim}{\sigma}^i$ denote the vector (6×1) of three-

Presented as Paper 79-0801 at the AIAA/ASME/ASCE/AHS 20th Structures, Structural Dynamics & Materials Conference, St. Louis, Mo., April 4-6, 1979; submitted May 11, 1979; revision received Dec. 4, 1979.

Index categories: Structural Composite Materials; Structural Durability.

*Research Scientist, School of Civil Engineering.

†Regents' Professor of Mechanics, School of Civil Engineering. Member AIAA.

dimensional stress in the ith layer, and let c^i be the compliance matrix of the ith layer (treated here as general anisotropic) in the element coordinates. (The compliance properties of each layer, in element coordinates, are assumed to be obtained from those in the layer-principal-material-directions through appropriate tensor transformations.) For the moment, let us assume that a candidate stress field is chosen such that it satisfies the three-dimensional stress-equilibrium equations, a priori, everywhere within each layer in each finite element. For the sake of generality, let us assume that this stress field does not satisfy the traction reciprocity conditions either at the interlayer interfaces within each element, or at the interelement boundaries of adjoining finite elements. (Later, in the details of the chosen stress field in the present formulation, it will be seen that the interlayer traction reciprocity condition is, however, satisfied a priori.) Let us also assume, for the present, that the chosen stress field does not satisfy the traction boundary conditions at $s^i_{\sigma n}$ a priori. (Again, it will be seen that in the details of the presently chosen stress field, the condition of vanishing tractions on the crack face are, for the most part, satisfied a priori.) Under these assumptions, it can be shown, following the basic theory of hybrid stress finite elements presented in Refs. 4, 6, and 7, that the conditions of compatibility of strains corresponding to the assumed stresses, the interelement and interlayer traction reciprocity conditions, and the traction boundary conditions follow from the variational principle, which is stated as the stationary condition of the following (modified) complementary energy functional:

$$\pi_{HS}(\sigma^i;u^i;u^i_\sigma) = \sum_{n=1}^{M}\Big[\sum_{i=1}^{k}\Big(\int_{V^i_n}\frac{1}{2}\sigma^{iT}c^i\sigma^i\,dV - \int_{\partial V^i_n - s^i_{\sigma n}} T^{iT}u^i\,ds - \int_{s^i_{\sigma n}}(T^{iT}-\bar{T}^{iT})u^i_\sigma\,ds\Big)\Big] \tag{1}$$

where u^i are Lagrange multipliers that are introduced to enforce the traction reciprocity condition at the interelement/interlayer interfaces; u^i_σ are another set of Lagrange multipliers to enforce the traction boundary conditions (b.c); $\bar{T}^i$ are prescribed tractions; and $\bar{T}^{iT}$ indicates the transpose of the vector $\bar{T}^i$, etc. The idea of introducing independent Lagrange multipliers u^i_σ to enforce traction b.c., as accurately as described, is detailed in Ref. 7. For purposes of conceptual clarity, imagine the domain of a cracked laminate to be descritized into finite elements as shown in Fig. 1, where a type 1 element is a "regular" element; type 2 is an element with the crack front as one of its edges, and hence has vanishing tractions on the crack face; and type 3 is an element which may have the crack front as one of its edges. In general, the three field variables in the functional of Eq. (1) can be assumed as

$$\sigma^i = P^i\beta + P^i_s\beta^i_s \text{ in } V^i_n (i=1,\ldots k;\ n=1,\ldots M) \tag{2}$$

$$u^i = L^i q^i \text{ at } \partial V^i_n \tag{3}$$

$$u^i_\sigma = L^i q^i + u^i_p \text{ at } S^i_{\sigma n} \tag{4}$$

from Eq. (2), the boundary tractions can be derived as

$$T^i = R^i\beta + R^i_s\beta^i_s \text{ at } \partial V^i_n \tag{5}$$

We note that in Eq. (4), u^i_p are point-wise Lagrange multipliers to enforce traction boundary conditions, as accurately as desired, using the collocation technique as detailed in Ref. 7. In Eq. (2), β are undetermined parameters in the assumed equilibrated stress field of a regular polynomial nature; while β^i_s are undetermined parameters in the assumed equilibrated stress field of singular (inverse square root from the crack front) nature. We draw attention here to the fact that the parameters β are common to all layers ($i=1,\ldots k$) within an element; this is due to the fact that as seen from the details to follow, the regular stress field in an element satisfies the interlayer traction reciprocity condition a priori, but not the interelement traction reciprocity condition. On the other hand, β^i_s are parameters which vary from layer to layer ($i=1,\ldots k$) within an element; and the interlayer reciprocity condition for tractions corresponding to the singular stress field is then satisfied by exactly matching the parameters β^i_s at the interlayer interfaces, as shown in the following. In Eq. (3) L^i are interpolation functions at the boundaries of ∂V^i_n such that the boundary displacement field u^i is uniquely interpolated in terms of generalized nodal displacements q^i.

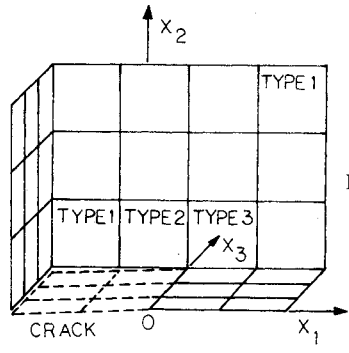

Fig. 1 Types of finite elements.

Even though Eqs. (2-5) were written in their most general form, we now note certain specific simplifications: 1) for type 1 (Fig. 1) "regular" elements, the stress field can be expected to be fairly smooth, and traction boundary conditions do not play a critical role; hence for these elements, we take $\beta^i_s=0$ and $u^i_p=0$; 2) for type 2 (Fig. 1) "singular" elements, the most general assumptions as in Eqs. (2-5) are used, and specifically for a stress-free crack face, $\bar{T}^i=0$; 3) for type 3 (Fig. 1) "singular" elements which do not share the stress-free crack face, the additional Lagrange multipliers u^i_p as in Eq. (4) are removed, i.e., $u^i_p=0$. The development of a "multilayer finite element" stiffness matrix follows fairly standard procedure, as detailed for instance in Refs. 4 and 6-8, and these details are omitted here. Since the crux of the present problem lies in a judicious choice of the field variables, the details of the specific choices made in the present work are given below.

Field Variables for Regular (Type 1) Elements

Consider x_α ($\alpha=1,2$) to be the in-plane coordinates of the laminate and x_3 to be the thickness coordinate. For Type 1 "regular" elements (denoted by superscript R), we start with the assumption for $\epsilon^R_{\alpha\beta}$ in the entire stack of layers in each finite element, as

$$\epsilon^R_{\alpha\beta} = \epsilon^{(0)}_{\alpha\beta} + X_3\epsilon^{(1)}_{\alpha\beta} + (X_3)^2\epsilon^{(2)}_{\alpha\beta} + (X_3)^3\epsilon^{(3)}_{\alpha\beta}\ (\alpha,\beta=1,2) \tag{6}$$

Further, each of the quantities $\epsilon^{(m)}_{\alpha\beta}$ ($m=0,1\ldots3$) is assumed as

$$\epsilon^{(m)}_{\alpha\gamma} = [1;X_1;X_2;X_1^2;X_1X_2;X_2^2]\{\beta^{(m)}_{\alpha\gamma}\} \tag{7}$$

where $\beta^{(m)}_{\alpha\gamma}$ are six undetermined parameters for each $m=0,1\ldots3$, and $\alpha\gamma=11$, 22, and 12. As seen from Eqs. (6) and (7), there are a total of 72 undetermined parameters β in the finite element comprising all of the layers. We assume that $\epsilon_{33}\simeq 0$.

The inplane stresses $\sigma^i_{\alpha\beta}$ within the ith layer are derived from $\epsilon^R_{\alpha\beta}$ as

$$\sigma^i_{\alpha\beta} = E^i_{\alpha\beta\gamma\delta}\epsilon^R_{\gamma\delta} \tag{8}$$

where $E^i_{\alpha\beta\gamma\delta}$ is the general anisotropic elasticity tensor, in element coordinates, corresponding to inplane stresses, for the ith layer. The transverse shear and normal stresses $\sigma_{\alpha3}$ and

σ_{33}, respectively, are obtained by integrating the equilibrium equations (ignoring body forces, for the present) as

$$\sigma^i_{\alpha 3} = -\int_{X_3} \sigma^i_{\alpha\beta,\beta} dx_3 \qquad (\alpha = 1,2) \tag{9}$$

and

$$\sigma^i_{33} = -\int_{X_3} \sigma^i_{3\beta,\beta} dx_3 \qquad (\beta = 1,2) \tag{10}$$

Substituting Eq. (8) into Eq. (9) and (10), one obtains

$$\sigma^i_{13} = [B^i_j(X_3) + C^i_j]\xi_j \; (j = 1,2,3) \tag{11}$$

$$\sigma^i_{23} = [B^i_j(X_3) + C^i_j]\xi_j \; (j = 4,5,6) \tag{12}$$

$$\sigma^i_{33} = [B^i_j(X_3) + C^i_j]\xi_j \; (j = 7) \tag{13}$$

where $\xi_1 = \xi_4 = \xi_7 = 1$; $\xi_2 = \xi_5 = X_1$; $\xi_3 = \xi_6 = X_2$; B^i_j are functions of X_3 in the ith layer; and C^i_j are integration constants. The constants of integration, C^i_j $(j = 1,...7;\ i = 1,...K)$ can be so chosen, a priori, that the traction reciprocity condition at the interlayer interfaces is satisfied exactly. Assuming that the lamina are of constant thickness, and that all the interlayer interfaces are perpendicular to the X_3 coordinate, this traction reciprocity condition reduces to $\sigma^+_{i3} = \sigma^-_{i3}$ $(i = 1,2,3)$ where + and − denote, arbitrarily, either side of the interlayer interface. We assume that the applied tractions on the bottom surface of the laminate, within each finite element, can be expressed as

$$\bar{\sigma}_{13} = A^0_j \xi_j \; (j = 1,...3); \bar{\sigma}_{23} = A^0_j \xi_j \; (j = 4,...6); \bar{\sigma}_{33} = A^0_j \xi_j \; (j = 7) \tag{14}$$

where A^0_j $(j = 1,...7)$ are known constants. Thus, the constants of integration in the bottom-most layer can be adjusted to reflect the above known tractions on the bottom surface of the laminate. Thus, the stress field, which satisfies the conditions of interlayer traction reciprocity as well as the boundary conditions on the bottom surfaces a priori, can be written, for each layer within each element, as

$$\sigma^i_{\alpha\beta} = E^i_{\alpha\beta\gamma\delta}\left(\sum_{m=0}^{3} (x_3)^m [1; x_1; x_2; x_1^2; x_1x_2; x_2^2] \{\beta^{(m)}_{\gamma\delta}\} \right) \tag{15}$$

$$\sigma^i_{13} = \left\{ B^i_j[x_3] - B^i_j[x_3^{(i-1)}] + \sum_{R=0}^{i-1} A^R_j \right\} \xi_j \; (j = 1,2,3) \tag{16}$$

$$\sigma^i_{23} = \left\{ B^i_j[x_3] - B^i_j[x_3^{(i-1)}] + \sum_{R=0}^{i-1} A^R_j \right\} \xi_j \; (j = 4,5,6) \tag{17}$$

$$\sigma^i_{33} = \left\{ B^i_j[x_3] - B^i_j[x_3^{(i-1)}] + \sum_{R=0}^{i-1} A^R_j \right\} \xi_j \; (j = 7) \tag{18}$$

where

$$A^R_j = B^R_j[x_3^{(R)}] - B^R_j[x_3^{(R-1)}]; \quad R = 1,...(k-1) \tag{19}$$

In the above, $x_3^{(i-1)}$ and $x_3^{(i)}$ are the coordinates of the bottom and top surfaces, respectively, of the ith layer (see Fig. 2).

The topology of a type 1 "regular" element is shown in Fig. 3. The boundary displacement field for this regular element is expressed uniquely in terms of the respective nodal displacements. For instance, along the side A-B-C in Fig. 3, the boundary displacements are assumed as

$$\begin{aligned} u^i_\alpha = &-\tfrac{1}{4}\xi(1-\xi)(1-\zeta)u^{(i-1)}_{\alpha A} + \tfrac{1}{2}(1-\xi)(1+\xi)(1-\zeta)u^{(i-1)}_{\alpha B} \\ &+ \tfrac{1}{4}\xi(1+\xi)(1-\zeta)u^{(i-1)}_{\alpha C} - \tfrac{1}{4}\xi(1-\xi)(1+\zeta)u^{(i)}_{\alpha A} \\ &+ \tfrac{1}{2}(1-\xi)(1+\xi)(1+\zeta)u^{(i)}_{\alpha B} + \tfrac{1}{4}\xi(1+\xi)(1+\zeta)u^{(i)}_{\alpha C} \end{aligned} \tag{20}$$

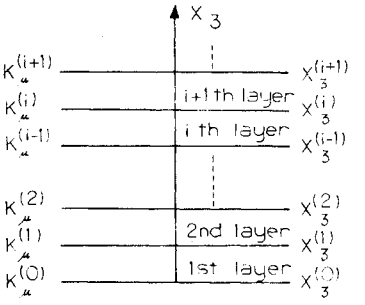

Fig. 2 Nomenclature for element variables.

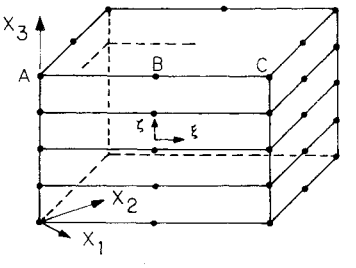

Fig. 3 Element topology.

and

$$u^i_3 = -\tfrac{1}{2}\xi(1-\xi)u_{3A} + (1-\xi)(1+\xi)u_{3B} + \tfrac{1}{2}\xi(1+\xi)u_{3C} \tag{21}$$

where u^i_α $(\alpha = 1,2)$ are inplane displacements, u^i_3 the transverse displacement, at the boundary of the ith layer; the superscripts $(i-1)$ and (i) denote the bottom and top surfaces of the layer, and $-1 \le \xi,\ \zeta \le 1$ are nondimensional coordinates at the boundary segment A-B-C, as indicated in Fig. 3. It is seen from Eq. (20) that the inplane displacement assumptions allow independent cross-sectional rotations of each layer; whereas the transverse displacement u_3 is constant through the thickness of laminate. Denoting by a, b and c, the number of parameters β, the number of element nodal displacements q, and the number of rigid body modes of the element, respectively, it is well known from the theory of hybrid-stress finite elements[7,8] that these parameters must obey the constraint, $b \le a + c$, in order to avoid spurious kinematic modes of the element. The number of nodal displacements corresponding to assumptions of the type given in Eqs. (20) and (21) can be seen to be, $b = 8(k+1)+4$ for a 4-noded (in the planform) element, whereas $b = 16(k+1)+8$ for an 8-noded (in the planform) element, where k = number of layers in the element. If the number of β's, i.e., a, is kept fixed at 72 as in Eq. (7), it is seen that the above inequality can be satisfied for a 4-noded element consisting of up to eight layers.

Field Variables for Singular (Types 2 and 3) Elements

The assumed stress field for these elements consists of both regular $(P^i\beta)$ and singular $(\tilde{P}^i_s\tilde{\beta}^i_s)$ terms. The regular variations are identical to those given in Eqs. (15-19). We now discuss the assumed equilibrated singular part, $(\tilde{P}^i_s\tilde{\beta}^i_s)$.

We first note that, in the present study, the angle-ply laminate is modeled such that each lamina is considered to be a homogeneous anisotropic medium. The problem of an anisotropic homogeneous body containing a through thickness crack and subject to plane symmetric, plane skew-symmetric, and antiplane shear loadings, has been treated by Sih and Liebowitz.[9] It is shown in Ref. 9 that the stress-singularity at the crack-tip is of the order of $(r^{-1/2})$. In generalizing the results in Ref. 9, two facts should be borne in mind: 1) satisfaction of the conditions on σ_{3i} (including the stress-free conditions) at the top and bottom surfaces of the laminate at the point of their intersection with the crack-front and 2) the effect of these stress-free conditions on the intensity factors for $\sigma_{\alpha\beta}$. It is also noted in this connection that studies by Hilton and Sih[10] indicate, for a cracked composite

laminate, that the stress σ^i_{33} near the crack-front is governed by a plane-strain condition in regions away from free-surfaces and interlayer surfaces. With these observations in mind, we present here a simple approach which ignores, a priori, the plane strain condition for the singular stress σ^s_{33}, and which facilitates the accurate enforcement of stress-free conditions ($\sigma^s_{3i}=0$, $i=1,2,3$) at the top and bottom surfaces of the laminate. In this process, we generalize the familiar metals based concepts of modes I, II, and III stress-intensity factors, and introduce several such factors in each of the stress components. For conceptual clarity, let the singular stress field in types 2 and 3 elements be represented by,

$$\underset{\sim}{\sigma}^{is} \equiv \underset{\approx}{P}^i_s \underset{\sim}{\beta}^i_s \quad (i=1,2...k) \tag{22}$$

where β^i_s can be called the vector of "stress-intensity factors" for the ith layer.

Let (r,θ,x_3) be cylindrical polar-coordinates centered at the crack-front, as shown in Fig. 1. We note that the assumed singular stress field σ^s_{ij} must satisfy the equilibrium equations, in the absence of body forces, as

$$(\sigma^{is}_{mn})_{,n}=0 \text{ and } \sigma^{is}_{mn}=\sigma^{is}_{nm} \quad (m,n=1,2,3;\ i=1,...k) \tag{23a,b}$$

We start by assuming σ^{is}_{33} in each layer ($i=1,...k$) as

$$\sigma^{is}_{33}=\frac{K^i_4(X_3)}{\sqrt{2\pi r}}\cos\frac{\theta}{2}+\frac{K^i_5(X_3)}{\sqrt{2\pi r}}\sin\frac{\theta}{2}$$

$$=K^i_4 Re[Z^{-1/2}]-K^i_5 \mathrm{Im}[Z^{-1/2}] \tag{24}$$

where $Z=X_1+iX_2=re^{i\theta}$. Note that K_4 and K_5 are functions of X_3. The third of the equilibrium equations, viz.,

$$\sigma^{is}_{3\alpha,\alpha}=-\sigma^{is}_{33,3} \tag{25}$$

is then solved by setting $\sigma^{is}_{3\alpha}=\sigma^{ish}_{3\alpha}+\sigma^{isp}_{3\alpha}$ where the additional superscripts h and p indicate the homogeneous and particular solutions, respectively. The particular solution of Eq. (25) can be obtained by setting,

$$\sigma^{isp}_{31}=\phi_{,2};\ \sigma^{isp}_{32}=\phi_{,1};\ \text{and}\ \phi=-\tfrac{1}{2}\iint\sigma^{is}_{33,3}dx_1dx_2 \tag{26}$$

In the present case, the crack is assumed to be present along the x_1 axis, with the crack face perpendicular to the x_2 axis. Thus σ^{is}_{32} must vanish at $\theta(\pm\pi)$ in the type 2 element (Fig. 1). Noting this fact, the solutions to Eq. (26) can be written as

$$\sqrt{2\pi}\sigma^{isp}_{31}=-K_{4,3}(r)^{1/2}\cos(\theta/2)+K_{5,3}(r)^{1/2}\sin(\theta/2) \tag{27}$$

and

$$\sqrt{2\pi}\sigma^{isp}_{32}=K_{4,3}\{(r)^{1/2}(-\sin\theta/2)+C\sqrt{|X_1|}\}$$

$$+K_{5,3}(r)^{1/2}(-\cos\theta/2) \tag{28}$$

where $K_{4,3}=\partial[K_4(x_3)]/\partial x_3$; $C=0$, $(-\pi/2)\le\theta\le(\pi/2)$; $C=1.0$, $(\pi/2)<\theta\le\pi$; and $C=-1.0$, $(-\pi)<\theta\le(-\pi/2)$. For $\sigma^{ish}_{3\alpha}$ ($\alpha=1,2$) we take the antiplane shear asymptotic solution for a cracked anisotropic solid, given in Ref. 9, as

$$\sigma^{ish}_{13}=-\frac{K^i_3(x_3)}{\sqrt{2\pi r}}Re\left[\frac{S^i_3}{(\cos\theta+S^i_3\sin\theta)^{1/2}}\right]$$

$$=\frac{-K^i_3(x_3)}{\sqrt{2\pi r}}Re[S^i_3 Z_3^{-1/2}] \tag{29}$$

and

$$\sigma^{ish}_{23}=\frac{K^i_3(x_3)}{\sqrt{2\pi r}}Re\left[\frac{1}{(\cos\theta+S^i_3\sin\theta)^{1/2}}\right]=\frac{K^i_3(x_3)}{\sqrt{2\pi r}}Re[Z_3^{-1/2}] \tag{30}$$

where, $Z_3=X_1+S^i_3X_2=r(\cos\theta+S^i_3\sin\theta)$; and S^i_3 is a complex number depending on the anisotropic elastic compliance coefficients of the lamina.[9] We now consider the first two equilibrium equations,

$$\sigma^{is}_{11,1}+\sigma^{is}_{12,2}=-\sigma^{is}_{13,3} \tag{31}$$

and

$$\sigma^{is}_{22,2}+\sigma^{is}_{12,1}=-\sigma^{is}_{23,3} \tag{32}$$

The particular solutions of Eqs. (31) and (32), respectively, can be obtained by setting,

$$\sigma^{isp}_{11}=-\int_{x_1}\sigma^{is}_{13,3}dx_1 \tag{33}$$

$$\sigma^{isp}_{22}=-\int_{x_2}\sigma^{is}_{23,3}dx_2 \tag{34}$$

and

$$\sigma^{isp}_{12}=0 \tag{35}$$

We note that on the crack face, i.e., at $\theta=\pm\pi$, $\sigma^{isp}_{22}=0$. Using this condition, and substituting for σ^{is}_{23} from Eqs. (28) and (30) into Eq. (34), we obtain

$$\sqrt{2\pi}\sigma^{isp}_{22}=K^i_{4,33}(r)^{3/2}\{-2/3(\cos3/2\theta)-C\sin\theta(|\cos\theta|)^{1/2}\}$$

$$+K^i_{5,33}(r)^{3/2}\{2/3(\sin3/2\theta)+2/3C(|\cos\theta|)^{3/2}\}$$

$$+K^i_{3,3}(r)^{1/2}\{-2Re[(1/S^i_3)(\cos\theta+S^i_3\sin\theta)^{1/2}]$$

$$+2C(|\cos\theta|)^{1/2}Re[i/S^i_3]\} \tag{36}$$

where, $K^i_{4,33}=\partial^2K^i_4/\partial x_3^2$; and C is defined in Eq. (28). Likewise, we obtain

$$\sqrt{2\pi}\sigma^{isp}_{11}=K^i_{4,33}(r)^{3/2}2/3(\cos3/2\theta)-K^i_{5,33}(r)^{3/2}2/3$$

$$\times\sin(3/2\theta)+K^i_{3,3}(r)^{1/2}\{2Re[S^i_3(\cos\theta+S^i_3\sin\theta)^{1/2}]\} \tag{37}$$

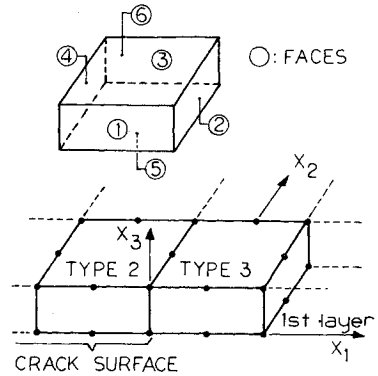

Fig. 4 Singular element topology.

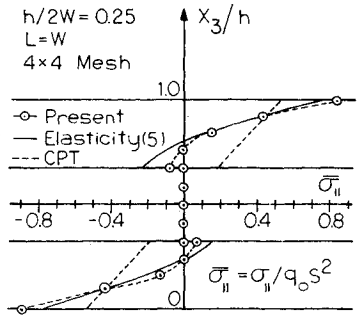

Fig. 5 Axial stress σ_{11} at $(X_1,X_2)=(L,L)$ [CPT: Classical laminated-plate theory].

For $\sigma^{ish}_{\alpha\beta}$ $(\alpha,\beta=1,2)$ we take the asymptotic solution for a cracked anisotropic solid,[9] as

$$\sigma^{ish}_{11}=\frac{K^i_1(x_3)}{\sqrt{2\pi r}}Re\left\{\frac{S_1S_2}{S_1-S_2}\left[\frac{S_2}{(\cos\theta+S_2\sin\theta)^{1/2}}-\frac{S_1}{(\cos\theta+S_1\sin\theta)^{1/2}}\right]\right\}+\frac{K^i_2(x_3)}{\sqrt{2\pi r}}Re\left\{\frac{1}{(S_1-S_2)}\times\left[\frac{S_2^2}{(\cos\theta+S_2\sin\theta)^{1/2}}-\frac{S_1^2}{(\cos\theta+S_1\sin\theta)^{1/2}}\right]\right\} \tag{38}$$

$$\sigma^{ish}_{22}=\frac{K^{(i)}_1(x_3)}{\sqrt{2\pi r}}Re\left\{\frac{1}{(S_1-S_2)}\left[\frac{S_1}{(\cos\theta+S_2\sin\theta)^{1/2}}-\frac{S_2}{(\cos\theta+S_1\sin\theta)^{1/2}}\right]\right\}+\frac{K^i_2(x_3)}{\sqrt{2\pi r}}Re\left\{\frac{1}{(S_1-S_2)}\times\left[\frac{1}{(\cos\theta+S_2\sin\theta)^{1/2}}-\frac{1}{(\cos\theta+S_1\sin\theta)^{1/2}}\right]\right\} \tag{39}$$

and

$$\sigma^{ish}_{12}=\frac{K^i_1(x_3)}{\sqrt{2\pi r}}Re\left\{\frac{S_1S_2}{(S_1-S_2)}\left[\frac{S_1}{(\cos\theta+S_1\sin\theta)^{1/2}}-\frac{S_2}{(\cos\theta+S_2\sin\theta)^{1/2}}\right]\right\}+\frac{K^i_2(x_3)}{\sqrt{2\pi r}}Re\left\{\frac{1}{(S_1-S_2)}\times\left[\frac{S_1}{(\cos\theta+S_1\sin\theta)^{1/2}}-\frac{S_2}{(\cos\theta+S_2\sin\theta)^{1/2}}\right]\right\} \tag{40}$$

In the above S_1 and S_2 (which, in fact should be written as S^i_1 and S^i_2 for $i=1,2...k$, but the superscript i is omitted for convenience) are complex numbers as defined in Ref. 9. By combining Eqs. (37) and (38), Eqs. (36) and (39), and Eqs. (35) and (40), respectively, we obtain the required solutions,

$$\sigma^{is}_{\alpha\beta}=\sigma^{ish}_{\alpha\beta}+\sigma^{isp}_{\alpha\beta}\quad(\alpha,\beta=1,2) \tag{41}$$

We note that the above derived singular field σ^{is}_{mn} $(i=1,...k;\ m,n=1,...3)$ identically satisfies, a priori, the traction boundary conditions on the crack face, namely, $\sigma^{is}_{2m}=0$ $(i=1,2,...k;\ m=1,2,3)$. As mentioned earlier, in type 2 elements, this singular field is augmented by regular polynomial functions $P^i\beta$. This regular field does not, in general, satisfy the crack-face condition that $\sigma^{iR}_{2m}=0$ $(i=1,...k;\ m=1,...3)$ in type 2 elements. The conditions of vanishing σ^R_{2m} on the crack-face in type 2 elements are enforced through a collocation technique (as detailed in Ref. 7), wherein the corresponding Lagrange multipliers are u^i_p as in Eq. (4). By increasing the number of collocation points (and hence the number u^i_p) on the crack-face, in type 2 elements, a high-degree of accuracy in the traction-free condition can be achieved, as seen from the present results as well as those in Ref. 7.

It remains to enforce: 1) the interlayer traction reciprocity conditions for σ^{is}_{mn}; 2) the traction boundary conditions including zero conditions for σ^{is}_{3m} $(m=1,2,3)$ at the top and bottom faces of the laminate; and 3) the conditions at the top surface of the laminate for the assumed regular field σ^{iR}_{3m} $(m=1,2,3)$. Conditions 3) are allowed to follow as natural b.c. from the variational principle of Eq. (4). However, conditions 1) and 2) above are satisfied exactly, a priori, as described below.

Each of the stress intensity factors within each layer, K^i_μ $(i=1,...k;\ \mu=1,2,...5)$ is interpolated using Hermitian polynomials as below:

$$K^i_\mu(X_3)=H_{00}(X_3)K^{(i-1)}_\mu+H_{10}(X_3)K^{(i-1)}_{\mu,3}+H_{01}(X_3)K^{(i)}_\mu+H_{11}(X_3)K^{(i)}_{\mu,3} \tag{42}$$

where $K^{(i)}_\mu$ and $K^{(i-1)}_\mu$ are, respectively, the values of K^i_μ at the top and bottom surfaces of the ith layer, $K^i_{\mu,3}=\partial[K^i_\mu]/\partial X_3$, and where,

$$H_{00}=1-3t^2+2t^3;\ H_{10}=(t-2t^2+t^3)h_i$$
$$H_{01}=3t^2-2t^3;\ H_{11}=(-t^2+t^3)h_i \tag{43}$$

where t is defined as $t=[X_3-X_3^{(i-1)}]/h_i$, $0\le t\le 1$. These values are shown in Fig. 2 for clarity.

Assuming that the lamina are of constant thickness and that X_3 is perpendicular to the interfaces, the interlayer continuity of the singular stresses σ^{is}_{3m} $(m=1,2,3)$ can easily be satisfied by equating the values of $(K^i_3, K^i_4$ and $K^i_5)$ and $(K^{i+1}_3, K^{i+1}_4, K^{i+1}_5)$ at the common interface. However, K^i_1 and K^i_2 which vary cubically within each ith layer, are allowed to be discontinuous at the interlayer interfaces. Further, assume that one of the surfaces, say the bottom surface, which the crack front intersects, is stress free. This stress free condition can be enforced by setting $K^{(0)}_3=K^{(0)}_4=K^{(0)}_{4,3}=K^{(0)}_{5,3}=0.0$. Finally, we note that since the stress-intensity parameters $K^{(i)}_\alpha$ and $K^{(i)}_{\alpha,3}$ $[\alpha=1,...5;\ i=0,...k]$, which form the vector β^s, are direct variables in the energy functional of Eq. (1), these can be computed directly as unknowns in the finite element equations.

Referring to Fig. 4 for the numbering of boundary surfaces of types 2 and 3 elements, the boundary displacement field, u^i of Eq. (3), is assumed as follows. For faces 1 and 2 of type 2 element and for faces 1 and 4 of type 3 element, the assumed field is

$$u^i_\alpha=a_{1\alpha}+a_{2\alpha}r^{1/2}+a_{3\alpha}r+a_{4\alpha}X_3+a_{5\alpha}X_3r^{1/2}+a_{6\alpha}X_3r\quad(\alpha=1,2) \tag{44}$$

and

$$u^i_3=a_7+a_8r^{1/2}+a_9r \tag{45}$$

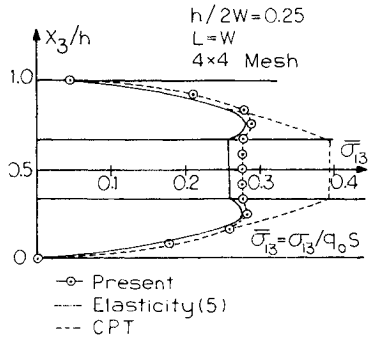

Fig. 6 Transverse shear stress σ_{13} at $(X_1,X_2)=(0,L)$ for a square plate $L=W$, $h/W=0.5$.

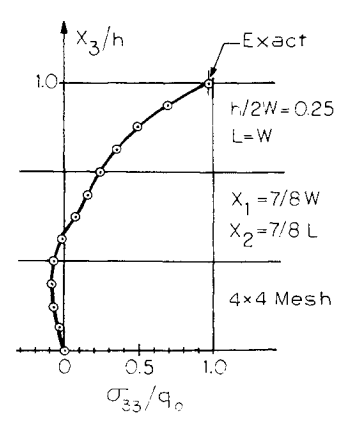

Fig. 7 Transverse normal stress σ_{33} at $(X_1/W, X_2/W)=(7/8, 7/8)$.

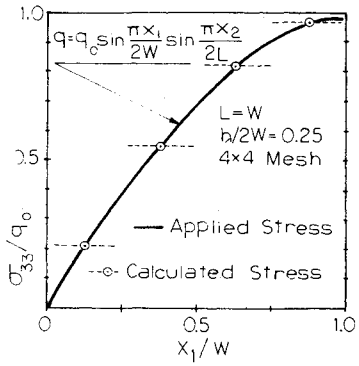

Fig. 8 Comparison of calculated σ_{33} at ($X_3=h$, and $X_2/L=7/8$) at various X_1 locations with applied transverse stress, q.

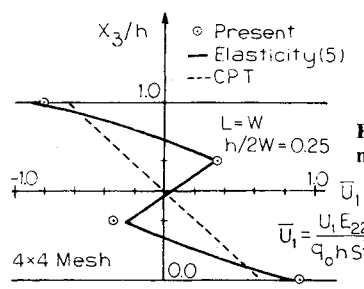

Fig. 9 Inplane displacement $u_1(X_3)$ at $(X_1,X_2)=(0,L)$.

In the above, r is the distance perpendicular to the crack front, i.e., $r=|x_1|$ on face 1 and $r=|x_2|$ on face 2 of the type 2 element. On faces 5 and 6 of the type 2 element, which are perpendicular to the crack front, the displacement field is assumed as

$$u_m^i = b_{1m}+b_{2m}X_1+b_{3m}X_2+b_{4m}r+b_{5m}r^{1/2}\cos(\theta/2)$$
$$+b_{6m}r^{1/2}\sin(\theta/2)+b_{7m}\cos(\theta/2)\sin^2(\theta/2)$$
$$+b_{8m}\sin(\theta/2)\cos^2(\theta/2) \quad (m=1,2,3) \tag{46}$$

In Eq. (46) $r=[(X_1)^2+(X_2)^2]^{1/2}$ and θ is the angle from crack-axis, as in Fig. 4. Noting that for the present finite element, there are 8 nodes at each interlayer surface, the above constants $a_{1\alpha}\ldots a_{6\alpha}$; $a_7\ldots a_9$, and $b_{1m}\ldots b_{8m}$ are expressed in terms of the yet unknown nodal displacements. Finally, the displacements at faces 3 and 4 of the type 2 element are assumed to be of the same form as in Eqs. (20) and (21) such that they are compatible with the boundary displacements of the neighboring elements.

Finally, we note that in the process of development of the element stiffness matrix based on Eq. (1), since the assumed singular σ^{is} is only equilibrated but does not correspond to compatible strain field a priori, it becomes necessary to numerically evaluate integrals of the type

$$I=\int_0^a\int_0^b f(r,\theta)\,dx_1 dx_2 \tag{47}$$

in a rectangular domain $0\le X_1\le a$; $0\le X_2\le b$; where r,θ are polar coordinates centered at $X_1=X_2=0$; and where $f(r,\theta)$ contains an $r^{-\alpha}$ type singularity ($0\le\alpha\le 1$). Special quadrature rules have been developed in the course of the present work to evaluate these integrals highly accurately. The details of these rules are given in Ref. 11, wherein further mathematical details of the present procedure are more fully elaborated upon.

Results and Discussion

A. Bending of a (0°/90°/0°) Laminate

The problem considered is that of bending of a simply supported, three-layer (0°/90°/0°), rectangular ($2W\times 2L$) laminate, under a transverse load [$q=q_0\sin(\pi X_1/2W)\sin(\pi X_2/2L)$ with the origin, $X_1=X_2=0$ being located at the lower left corner of the rectangle] applied at the top surface of the plate, for which an exact three-dimensional solution is available.[5] The properties of each lamina are (in the lamina principal material directions): $E_{11}=25\times 10^6$ psi; $E_{22}=10^6$ psi; $E_{33}=10^6$ psi; $G_{12}=5\times 10^5$ psi; $G_{23}=2\times 10^5$ psi; and $\nu_{12}=\nu_{13}=\nu_{23}=0.25$. The problem was solved for various values of the parameters, $S=(2W/h)$, where h is the laminate-thickness. Because of the geometric, material, and loading symmetries, only a quarter of the plate was modeled, with ($N\times M$) finite element (i.e., N and M elements, respectively, along the X_1 and X_2 directions). The convergence studies for various values of S, N, and M are included in Ref. 11, but are not given here due to space reasons; however, these results indicate that the present method converges excellently for both thick ($S\simeq 4$) as well as thin $S\ge 10$ laminates. Also, the rates of convergence were observed to be faster than those indicated in Ref. 2. We present here only the results for a thick laminate with $S=(2W/h)=4.0$; $L=W$; and when the laminate was modeled by a (4×4) finite element mesh (each finite element consisting of the entire stack of lamina).

The variation of σ_{11} with the thickness coordinate (X_3) at the edge of the plate ($X_1=0$; $X_2=L$) is shown in Fig. 5 along with the exact solution. The variation of σ_{13} with X_3 at the location ($X_1=L$; $X_2=L$) is shown in Fig. 6 along with the exact solution. Likewise, the variation of σ_{33} with X_3 at $[X_1=X_2=(7/8)L]$ is shown in Fig. 7. The variation of the computed σ_{33} at the top surface of the plate, along the X_1 coordinate, is shown in Fig. 8 for $X_2=(7/8)L$, and this variation is seen to agree excellently with the applied stress q; thus indicating that the satisfaction of traction boundary conditions is being accomplished excellently in the present assumed stress finite element procedure. Finally, the thickness-variation of inplane displacements at ($X_1=0$ and $X_2=L$) is shown in Fig. 9, from which it can be seen that the present boundary-displacement assumptions, which allow for the independent cross-sectional rotations of each layer, yield results in excellent accord with the exact three-dimensional elasticity theory. The above results may illustrate the accuracy and efficiency of the present method for an analysis of the three-dimensional stress state in uncracked laminates under general loading.

B. Through-the-Thickness Edge-Crack in a (0°/90°/90°/0°) Laminate

The geometry of the cracked laminate is shown in Fig. 10; with $(L/W)=1.0$; $(a/W)=0.2$; $(h_0/W)=(1/300)$; $h=4h_0$; $W=1.5$ in. The ply elastic constants (in the principal material directions) which are typical of a medium modulus graphite/epoxy, are chosen to be: $E_{11}=18.25\times 10^6$ psi; $E_{22}=1.5\times 10^6$ psi; $E_{33}=1.5\times 10^6$ psi; $G_{12}=G_{13}=G_{23}=0.95\times 10^6$ psi; $\nu_{12}=\nu_{23}=\nu_{13}=0.24$. The above problem definition is identical to the one in Ref. 3. A uniformly distributed stress is applied at the boundaries, $X_2=\pm L$; and the top and bottom surfaces of the laminate ($X_3=0$, and $4h_0$) as well as the crack-face, are assumed to be traction-free. Because of the appropriate geometric, material, and loading symmetries only a quarter of the plate bounded by $-a\le X_1\le(W-a)$; $0\le X_2\le L$; and $0\le X_3\le 2h_0$, need to be modeled. It is noted that in Ref. 3, the solution is obtained in two stages; one with a coarse mesh and the second with a very fine mesh for a substructure near the crack front. Thus, in Ref. 3, the coarse mesh consisted of $(9\times 18\times 2)$ elements (i.e., 9, 18, and 2 elements in X_2, X_1, and X_3 directions, respectively) in the quarter-plate with 570 nodes and 1710 degrees-of-freedom; while the inner mesh consisted of a $(11\times 19\times 4)$ finite element mesh (in X_2,X_1,X_3 directions, respectively) with 3600 degrees-of-freedom. In contrast, the present solution is obtained in a single stage using a $(11\times 7\times 1)$ finite element mesh (in X_1,X_2, and X_3 directions, respectively), in

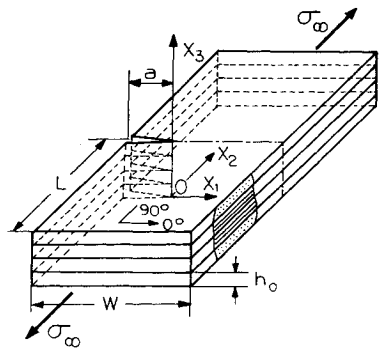

Fig. 10 Geometry of cracked laminate.

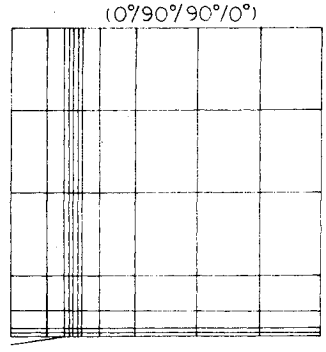

Fig. 11 Finite element model of cracked laminate.

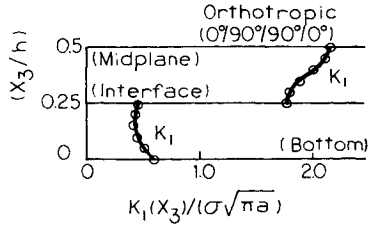

Fig. 12 Variation of K_1 through the thickness of lamiante.

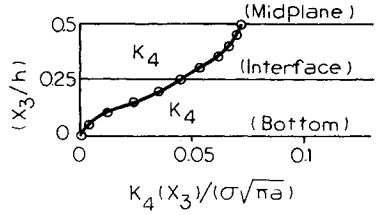

Fig. 13 Variation of K_4 through the thickness of laminate.

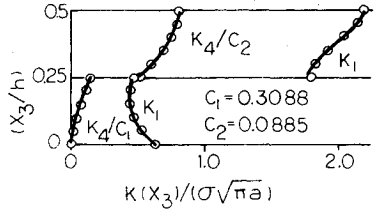

Fig. 14 Comparison of actual and nominal-plane-strain conditions.

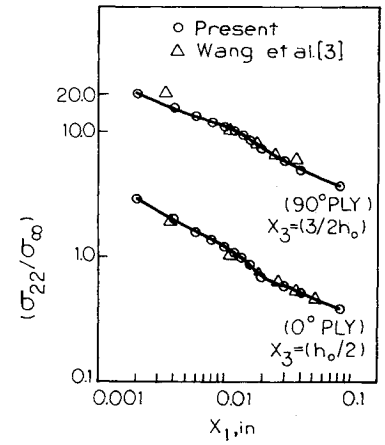

Fig. 15 Variation of σ_{22} (with X_1) near the crack front.

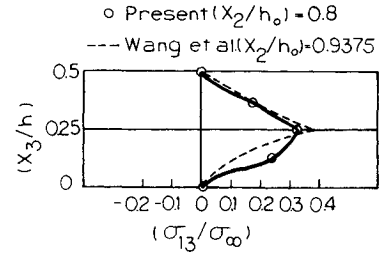

Fig. 16 Variation of σ_{13} with X_3 at ($X_1 = 0$, $X_2 = 0.8\ h_0$).

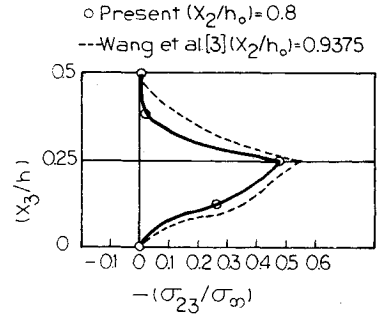

Fig. 17 Variation of σ_{23} with X_3 at ($X_1 = 0$, $X_2 = 0.8\ h_0$).

the quarter plate as shown in Fig. 11, with a total of 1562 degrees-of-freedom.

The values of the normalized stress intensity factors K_1^i (which are directly computed in the present procedure) and their variation with X_3 are shown in Fig. 12. As can be expected, there is a discontinuity in K_1 value at the interface between 0 and 90° plies, and moreover, the K_1 value is much higher in the 90° ply than in the 0° ply. The stress intensity factor K_4^i in the transverse normal stress σ_{33}^i, and its variation with X_3, is shown in Fig. 13. Note that K_4 is zero (actually set to zero) at $X_3 = 0$, is continuous at the interface between 0 and 90° plies, and its magnitude is much smaller than that of K_1.

It is also noted that in the present example, the factors K_2^i, K_3^i, and K_5^i were found to be nearly zero, as can be expected. If plane-strain conditions are assumed to prevail in each layer, it can be shown that in each ith layer, $K_1^i = (K_4^i/C_i)$ where C_i is a material constant for the general anisotropic medium. This material constant C_i can be derived in a straightforward manner for an anisotropic medium (and is equal to 2ν in the isotropic case, ν = Poisson ratio), and is given in Ref. 11. A comparison of K_1^i, and K_4^i/C_i is shown for each of the 0 and 90° layers in Fig. 14, which suggests that for this thin laminate ($W/h = 75$; $a/h = 15$), plane-strain conditions are not attained even at the interior of the laminate, away from free surfaces, or away from the lamina interfaces. However, results for thick isotropic and anisotropic laminates (which are given in Ref. 11, but not here, due to space reasons) do indicate that K_4 and K_1 meet the plane strain requirement at the interior of the laminate, away from free surfaces. However, the results for stress-intensity factor variations are not given in Ref. 3, because the procedure used therein does not permit a direct extraction of these factors in a convenient manner.

The distribution of inplane stress σ_{22}^i (normal to crack-axis), at the midplane of each ply, along X_1 (near the crack front) is shown in Fig. 15, along with comparison results in Ref. 3, which are noted to correlate excellently with the present results. Similar correlation between present results, for the other inplane stresses (not shown here, for want of space) both as functions X_1 and X_2 near the crack-front, and those in Ref. 3, was noted. The distribution of interlaminar shear stresses σ_{13} (X_3) and σ_{23} (X_3) along the

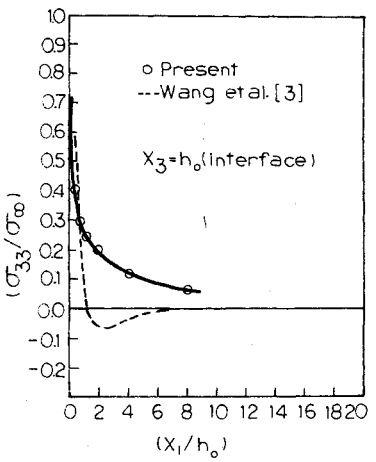

Fig. 18 Variation of σ_{33} with X_1 at ($X_2=0$, $X_3=h_0$).

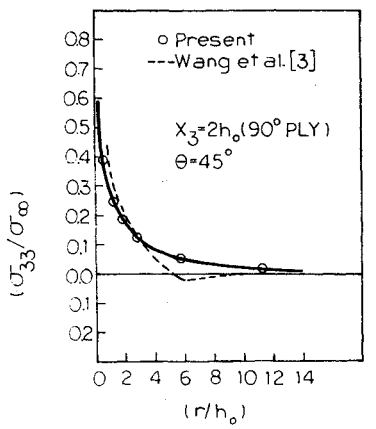

Fig. 19 Variation of σ_{33} with r at ($\theta=45°$, $X_3=2h_0$).

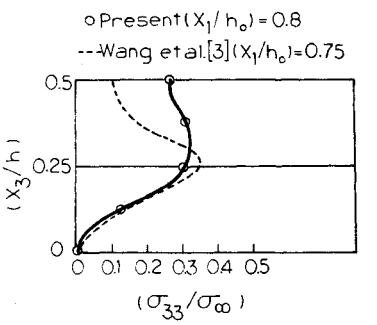

Fig. 20 Variation of σ_{33} with X_3 at ($X_1=0.8h_0$, $X_2=0$).

thickness coordinate at the location $[(X_2/h_0)=0.8$ and $X_1=0]$ are shown in Figs. 16 and 17 respectively; once again, good correlation is obtained between present results and those in Ref. 3. Figure 18 shows the variation of σ_{33} as a function of (X_1/h_0) at $(X_3/h_0)=1.0$ (interface); while Fig. 19 shows σ_{33} as a function of the radial distance (r/h_0) along a direction at 45 deg to the crack-axis at $(X_3/h_0)=2.0$ (midplane of laminate). It should be remarked here that in the present procedure, σ^i_{33} has a $(1/\sqrt{r})$ singularity built into it, while the solution in Ref. 3 is based on the use of regular polynomial stress fields. Finally, the variation of σ_{33} with the thickness coordinate X_3, at the location along the crack axis, $(X_1/h_0)=0.8$, are shown in Fig. 20 along with comparison results from Ref. 3, except at $(X_1/h_0)=0.75$. The present results were observed to predict a higher value of σ_{33}, in general, as seen from the specific case in Fig. 20; further, as seen from Fig. 18 the present results indicate no sign reversal in σ_{33} at the interface, at short distances from the crack tip, as in Ref. 3.

Summary

Considering the features: 1) that the present solution method leads to a direct evaluation of stress-intensity factors (and their variation in the laminate thickness direction) in the three-dimensional stress field, σ^i_{mn}, in each ith ply and 2) in the specific example treated here, that accurate results for details of stress-fields are obtained more economically (i.e., in a one-step solution with 1562 degrees-of-freedom in the present work, as contrasted to a two-step solution with (1710 + 3600) d.o.f. in previously reported Ref. 3 procedures); it appears that the presently reported "multilayer hybrid crack element" procedure offers a viable tool for stress as well as fracture analyses of laminates. Moreover, the procedure offers new and convenient ways for accounting for stress-singularities in all the six stress components σ^i_{mn} in each layer, their variation through the thickness of each ply, and the effects of free surfaces (normal to the crack-front) on these stress-intensity factor variations. The implication of the present results in formulating mechanisms for initiation of fracture, and subsequent subcritical damage in cracked laminates, is the object of our work in progress.

Acknowledgment

This work was supported by the U.S. AFOSR under Contract No. F49620-78-C-0085 with the Georgia Institute of Technology (G.I.T.) and by supplemental funds from G.I.T. The authors gratefully acknowledge this support. The authors also which to thank J. D. Morgan III for his timely encouragement during the course of this work.

References

[1] Wang, S. S., Mandell, J. F., and McGarry, F. J., "A Multilayer Hybrid-Stress Finite Element Analysis of a Through-Thickness Edge Crack in a ±45° Laminate," *Engineering Fracture Mechanics*, Vol. 9, 1977, pp. 217-238.

[2] Mau, S. T., Tong, P., and Pian, T.H.H., "Finite Element Solutions for Laminated Thick Plates," *Journal of Composite Materials*, Vol. 6, 1972, pp. 304-311.

[3] Wang, S. S., Mandell, J. F., and McGarry, F. J., "Three-Dimensional Solution for a Through-Thickness Crack in a Cross-Plied Laminate," *Fracture Mechanics of Composites*, ASTM STP 593, American Society for Testing and Materials, 1975, pp. 36-60.

[4] Pian, T.H.H., "Derivation of Element Stiffness Matrices by Assumed Stress Distributions," *AIAA Journal*, Vol. 2, 1964, pp. 1333-1336.

[5] Pangano, N. J., "Exact Solutions for Rectangular Bidirectional Composites and Sandwich Plate," *Journal of Composite Materials*, Vol. 4, 1970, pp. 20-34.

[6] Atluri, S. N., "On Hybrid Finite Element Models in Solid Mechanics," *Advances in Computer Methods for Partial Differential Equations*, R. Vichnevetsky, editor) AICA, Rutgers Univ., New Brunswick, N.J., 1975, pp. 346-356.

[7] Atluri, S. N. and Rhee, H. C., "Traction Boundary Conditions in Hybrid-Stress Finite Element Model," *AIAA Journal*, Vol. 16, May 1978, pp. 529-531.

[8] Pian, T.H.H. and Tong, P., "Finite Element Methods in Continuum Mechanics," *Advances in Applied Mechanics*, Vol. 12, edited by C. S. Yih, Academic Press, New York, 1972, pp. 2-53.

[9] Sih, G. C. and Liebowitz, H., "Mathematical Theories of Brittle Fracture," *Fracture Vol. 2*, edited by H. Liebowitz, Academic Press, New York, 1968, pp. 68-188.

[10] Hilton, P. D. and Sih, G. C., "Three-Dimensional Analysis of Laminar Composities with Through Cracks," *Fracture Mechanics of Composites*, ASTM STP 593, American Society for Testing and Materials, 1975, pp. 3-35.

[11] Nishioka, T. and Atluri, S. N., "An Efficient Assumed Stress Finite Element Procedure for Fracture Analysis of Multilayer Anisotropic Laminates," Georgia Institute of Technology, Tech. Report, 1979, in preparation.